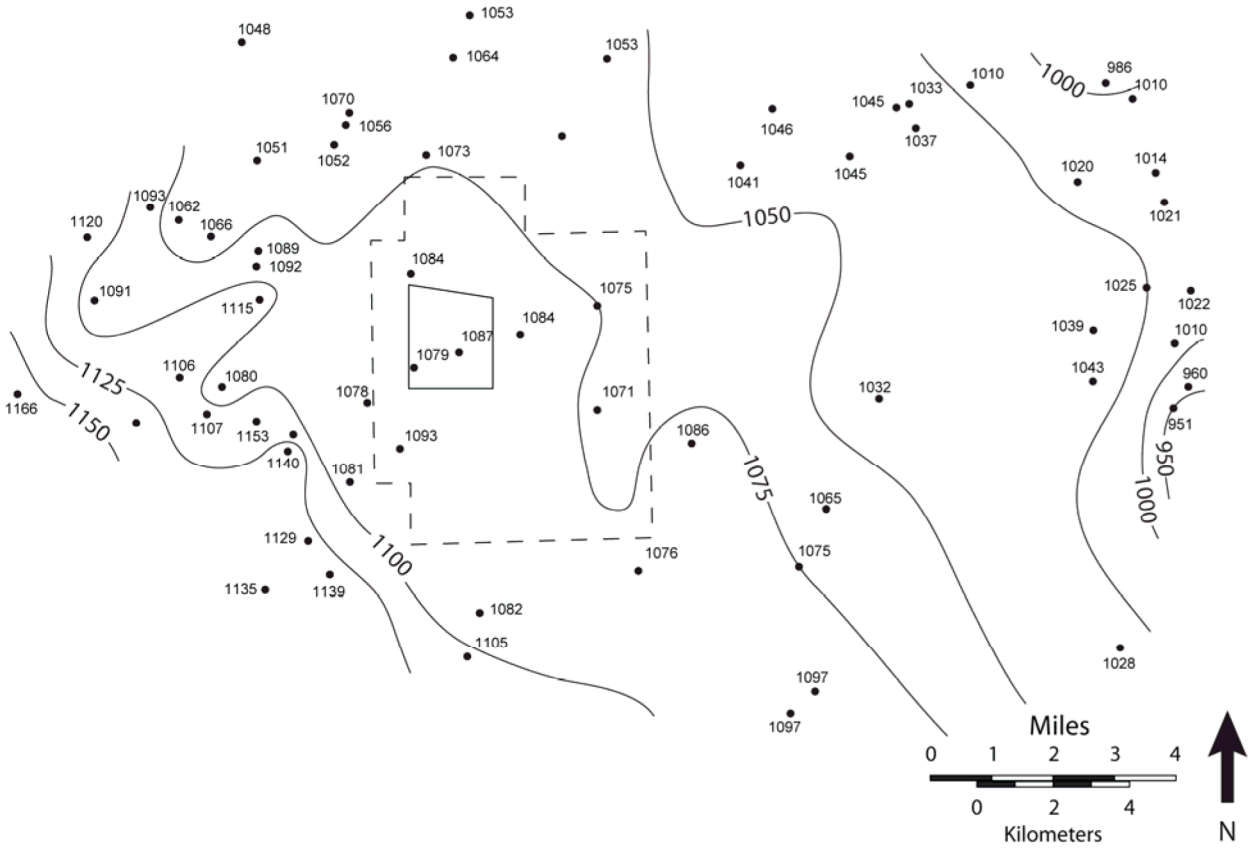

Figure 18 – Thickness (ft) of the Salado Formation, including the interval in Figure 17.

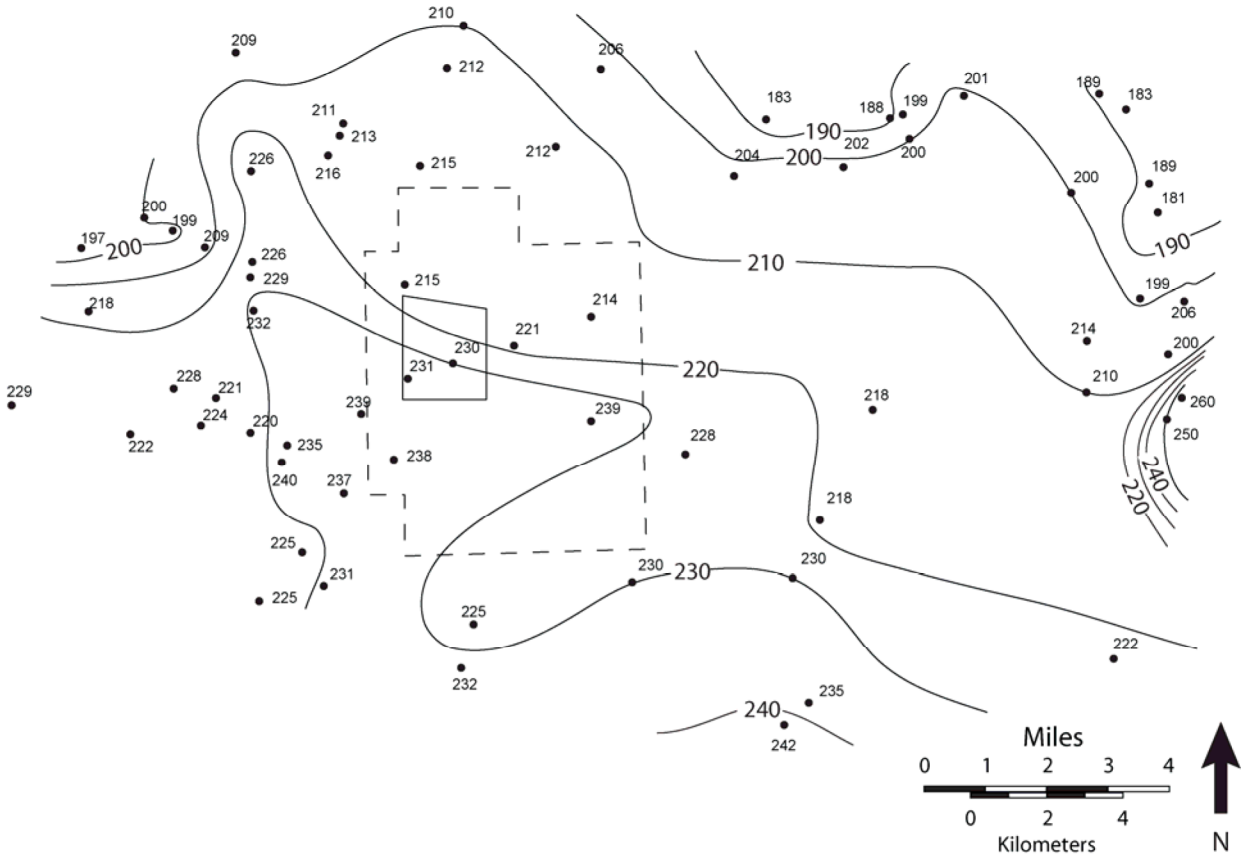

Figure 19 – Thickness (ft) of the Rustler Formation.

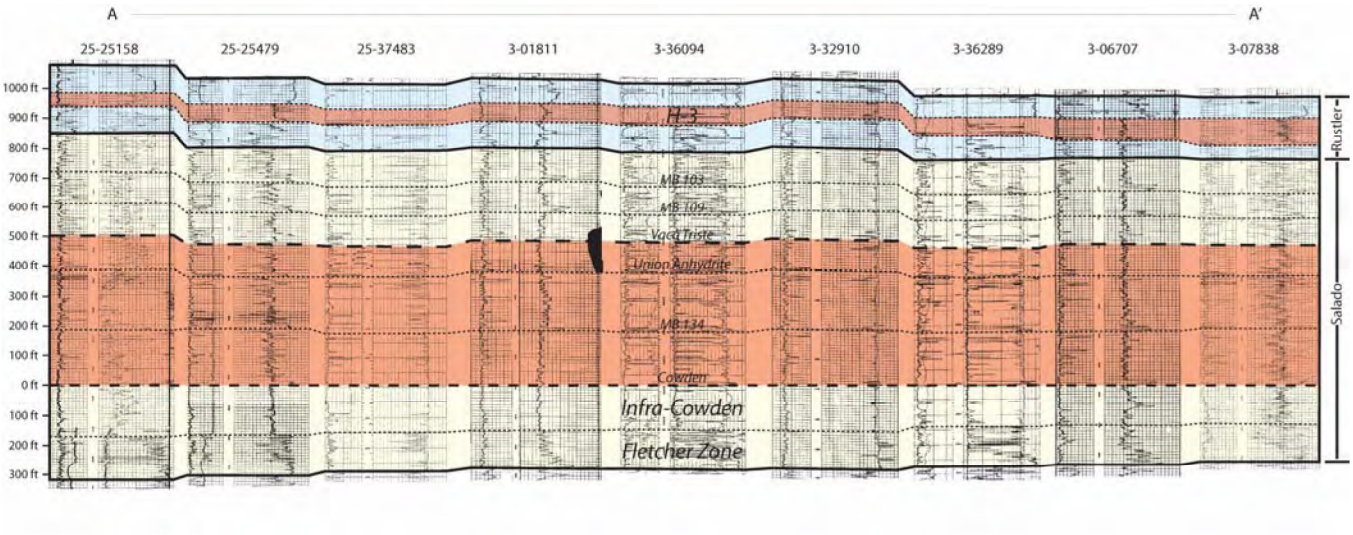

Figure 20 – West to east stratigraphic relationships across the study area and WCS facility from geophysical logs (not spaced to horizontal scale). See Figure 13 for locations. Different intervals are color coded for easier tracking. The black spot near the center is from the original scanned log.

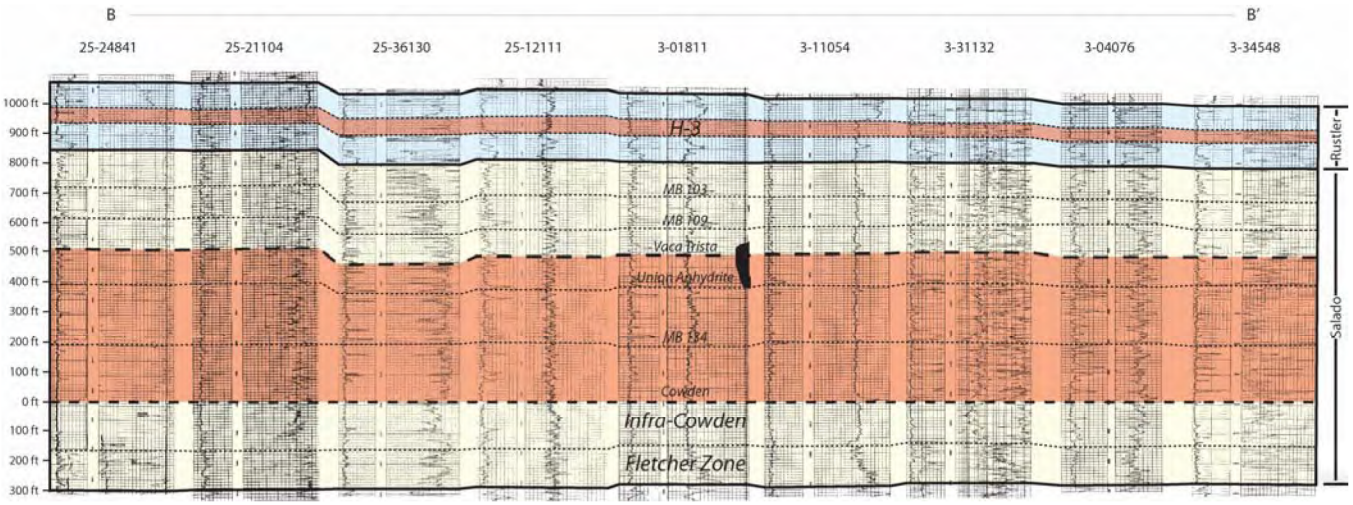

Figure 21 – South to north stratigraphic relationships across the study area and WCS facility from geophysical logs (not spaced to horizontal scale). See Figure 13 for locations. Different intervals are color coded for easier tracking. The black spot near the center is from the original scanned log.

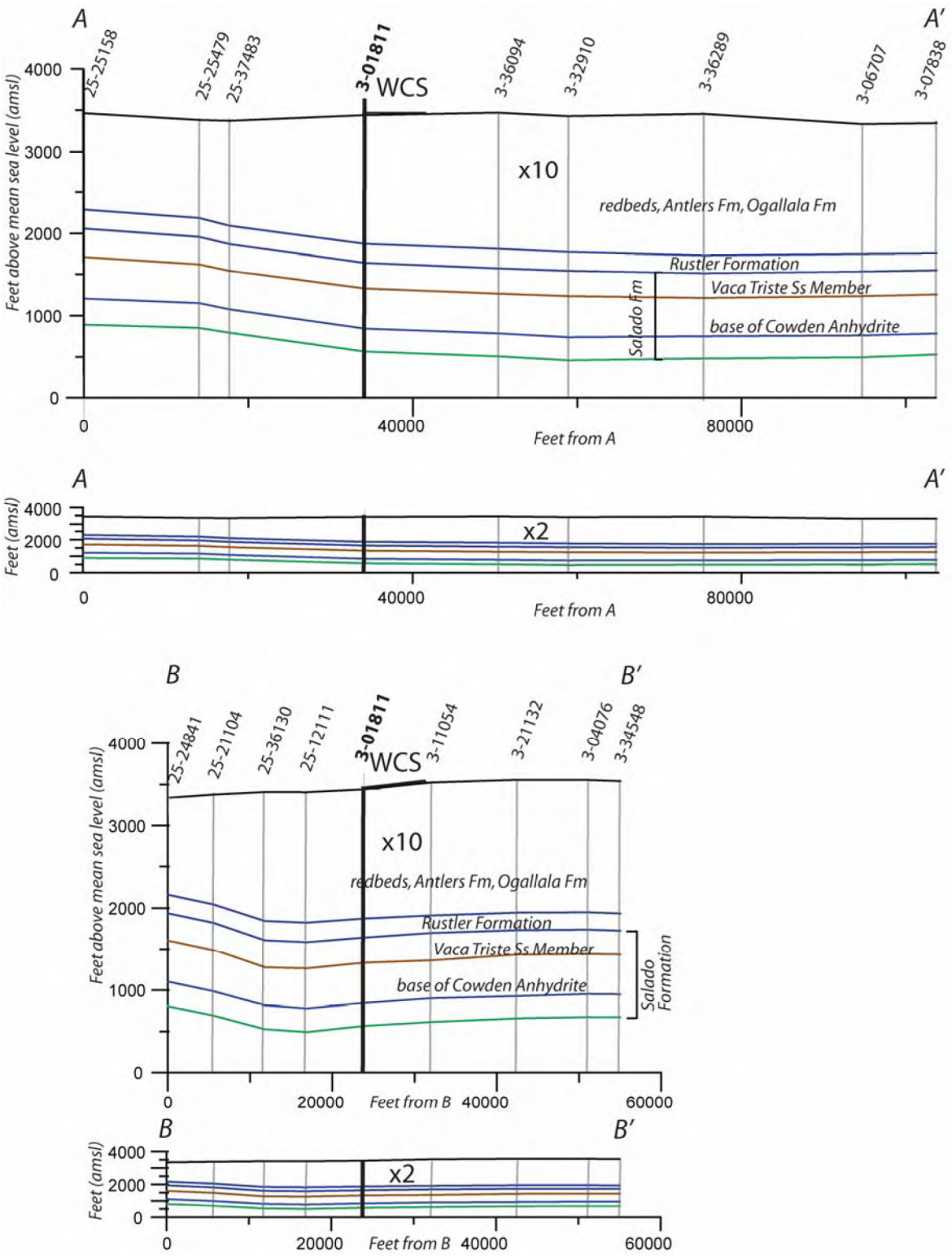

Figure 22 – Line drawings of elevation changes along cross-section A-A' (Figure 20) and B-B' (Figure 21) showing vertical exaggerations of 2 (lower graphics) and 10 (upper graphics). Horizontal scale is in feet measured from one end of the cross-section.

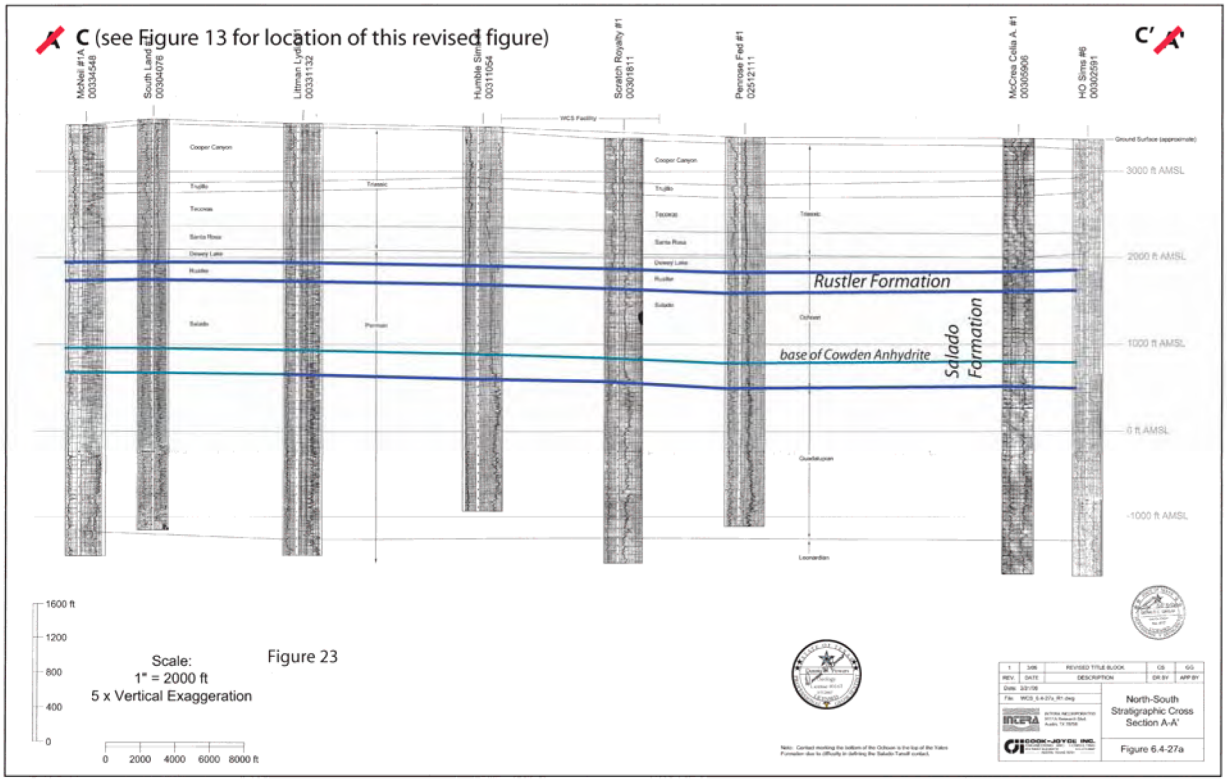

Figure 23 – Re-interpreted stratigraphic contacts (blue) for the Rustler and Salado Formations and base of Cowden Anhydrite (green) on cross-section (A-A') originally included in the application. A larger paper print of this figure is included in a pocket for this report.

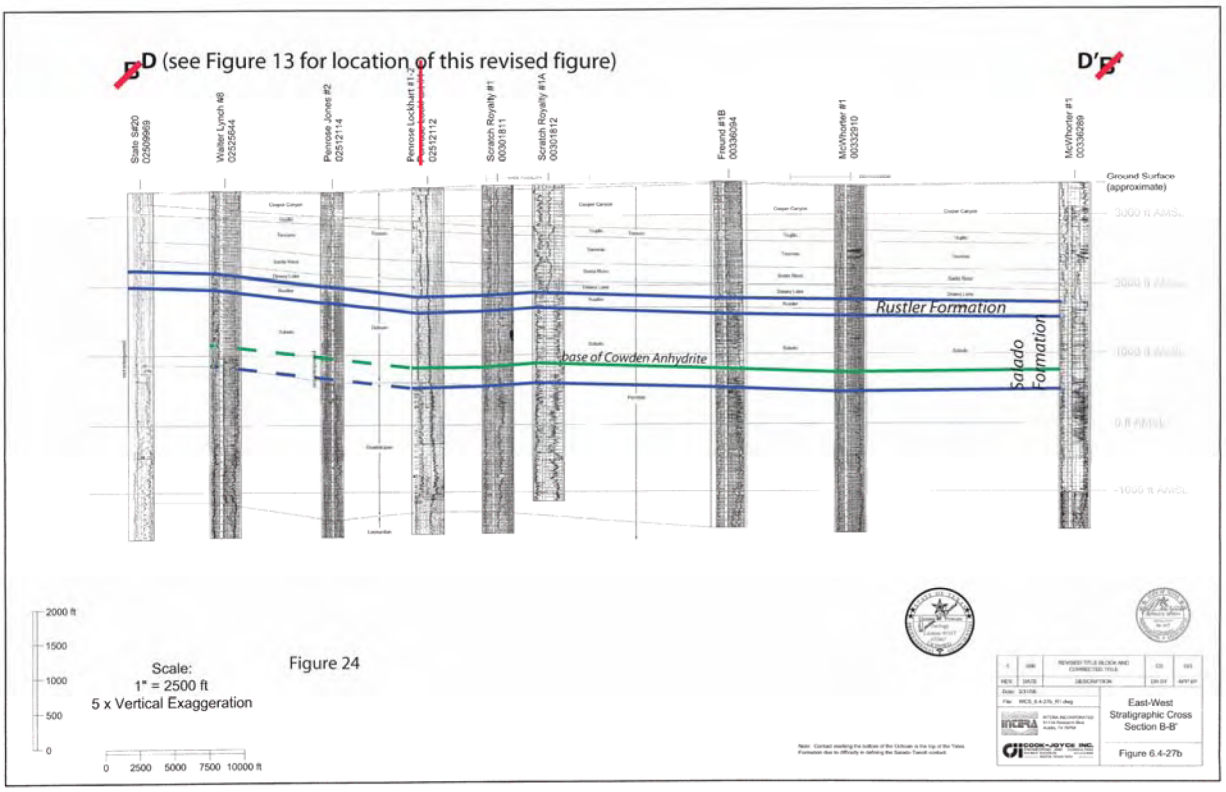

Figure 24 – Re-interpreted stratigraphic contacts (blue) for the Rustler and Salado Formations and base of Cowden Anhydrite (green) on cross-section (B-B') originally included in the application. A larger paper print of this figure is included in a pocket for this report.

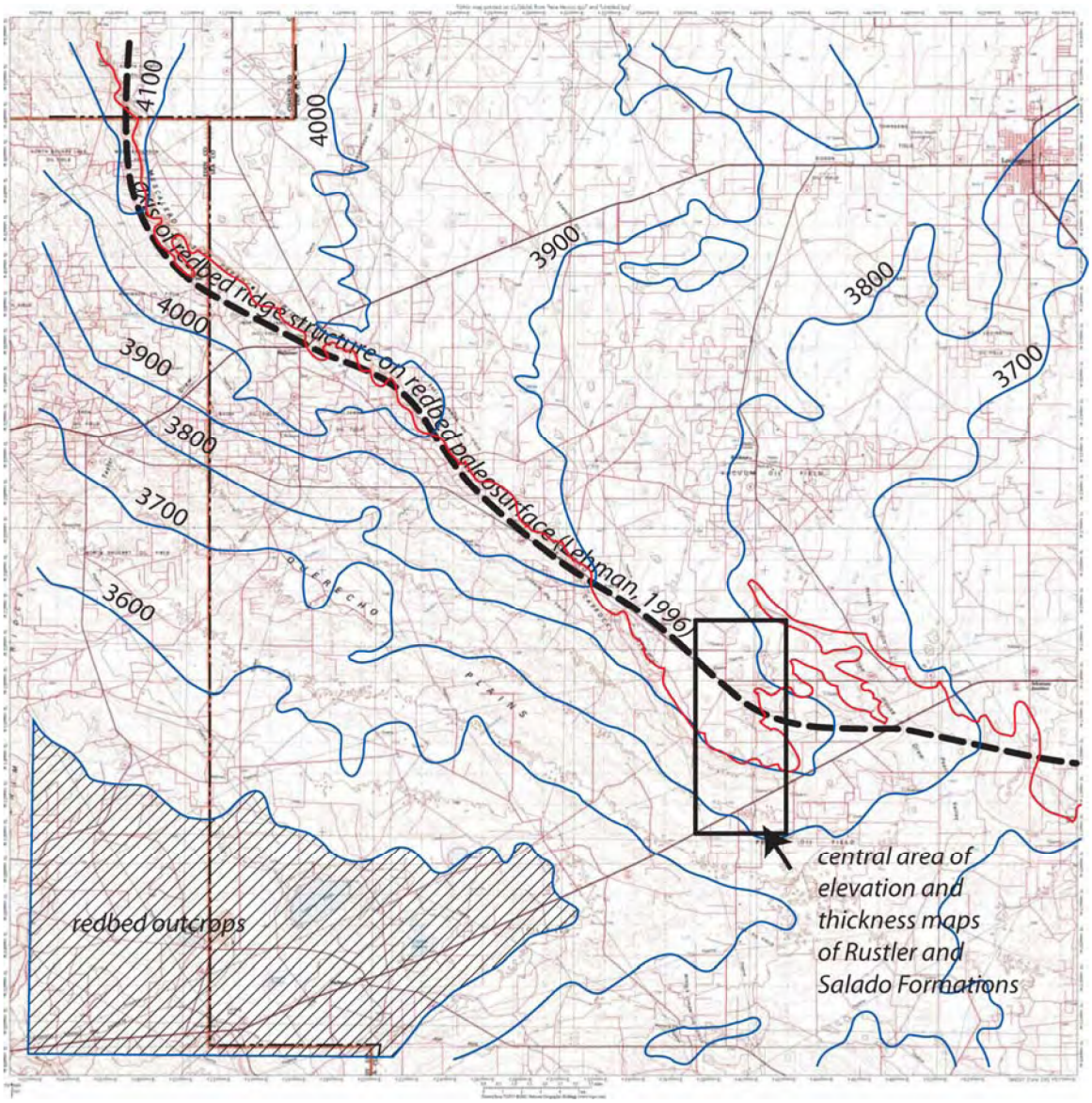

Figure 25 – The "redbed ridge" area in southeastern New Mexico shows contours (100 ft interval) of the elevation of the top of pre-Cretaceous redbeds and the axis (dashed line) of the "folding" based on Lehman (1996). The redbed ridge has been interpreted as a feature developed in response to dissolution of halite. The rectangle near the center identifies the central area of elevation and isopach maps (Figures 23-25) used to compare Rustler stratigraphic and isopach data with the elevation on the redbed paleosurface.

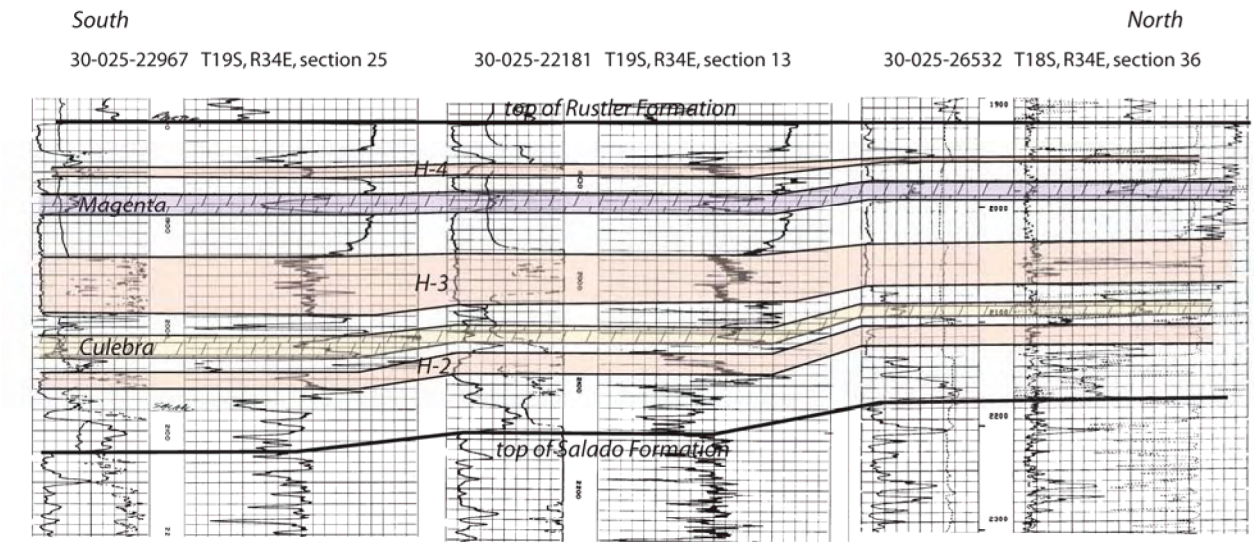

Figure 26 – Three geophysical logs illustrate persistent stratigraphic relationships of the Rustler Formation perpendicular to the trend of the redbed ridge. The formation thins consistently to the northeast (Figure 29).

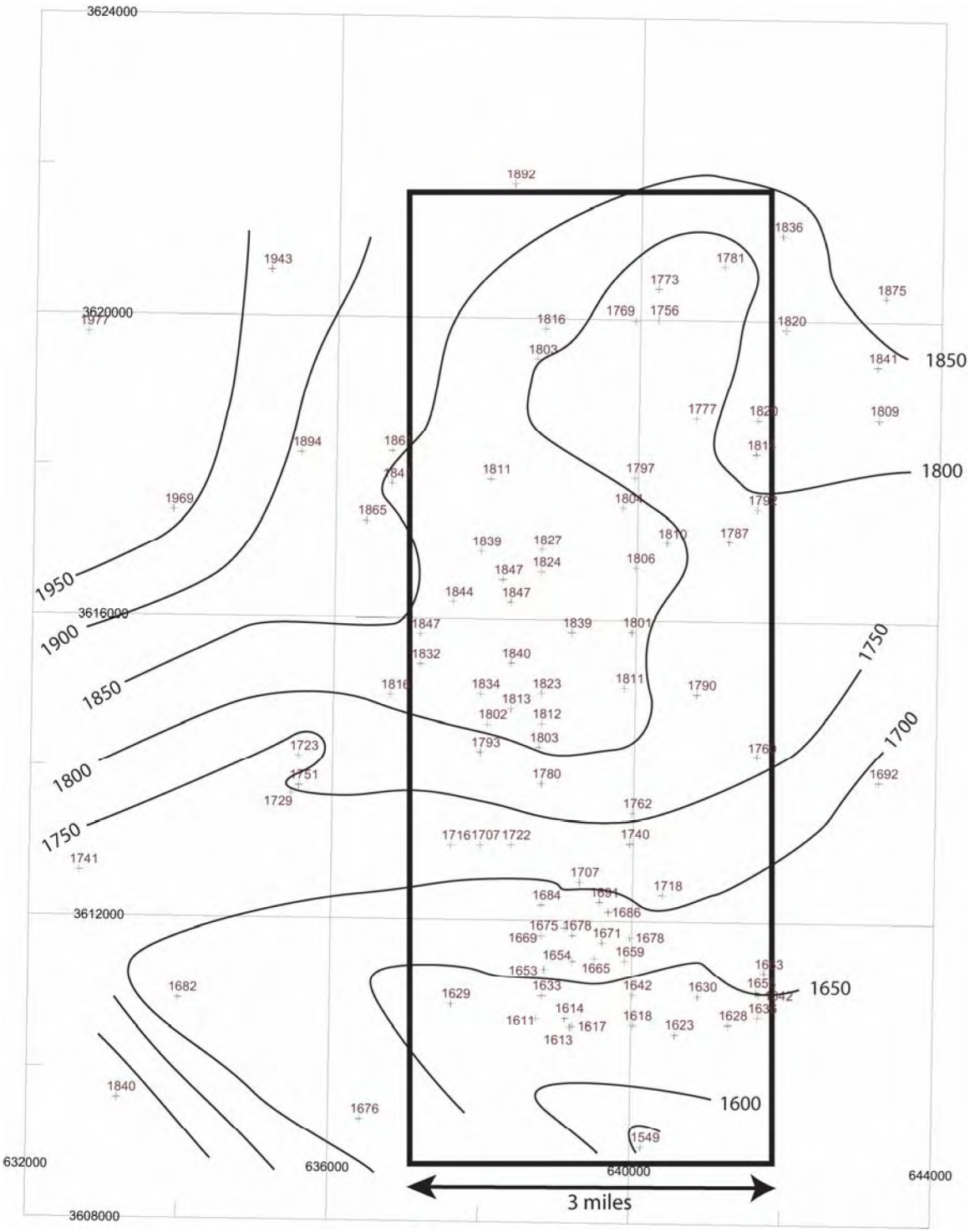

Figure 27 – Elevation (ft amsl) for the top of the Salado across the trend of the redbed ridge. Gridlines are UTM coordinates (m; Zone 13). Rectangle is shown in Figure 25.

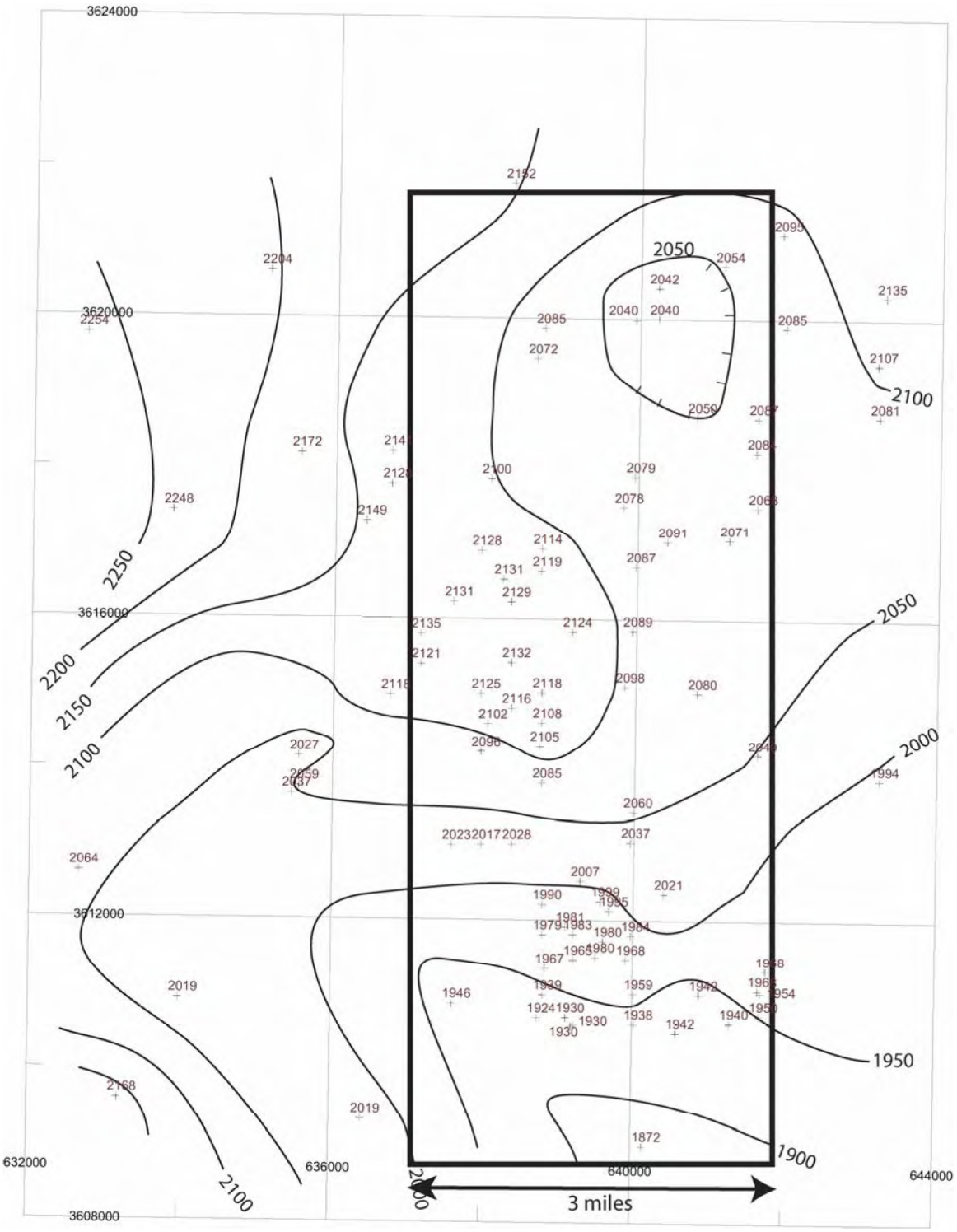

Figure 28 – Elevation (ft amsl) for the top of the Rustler across the trend of the redbed ridge. Gridlines are UTM coordinates (m; Zone 13). Rectangle is shown in Figure 25.

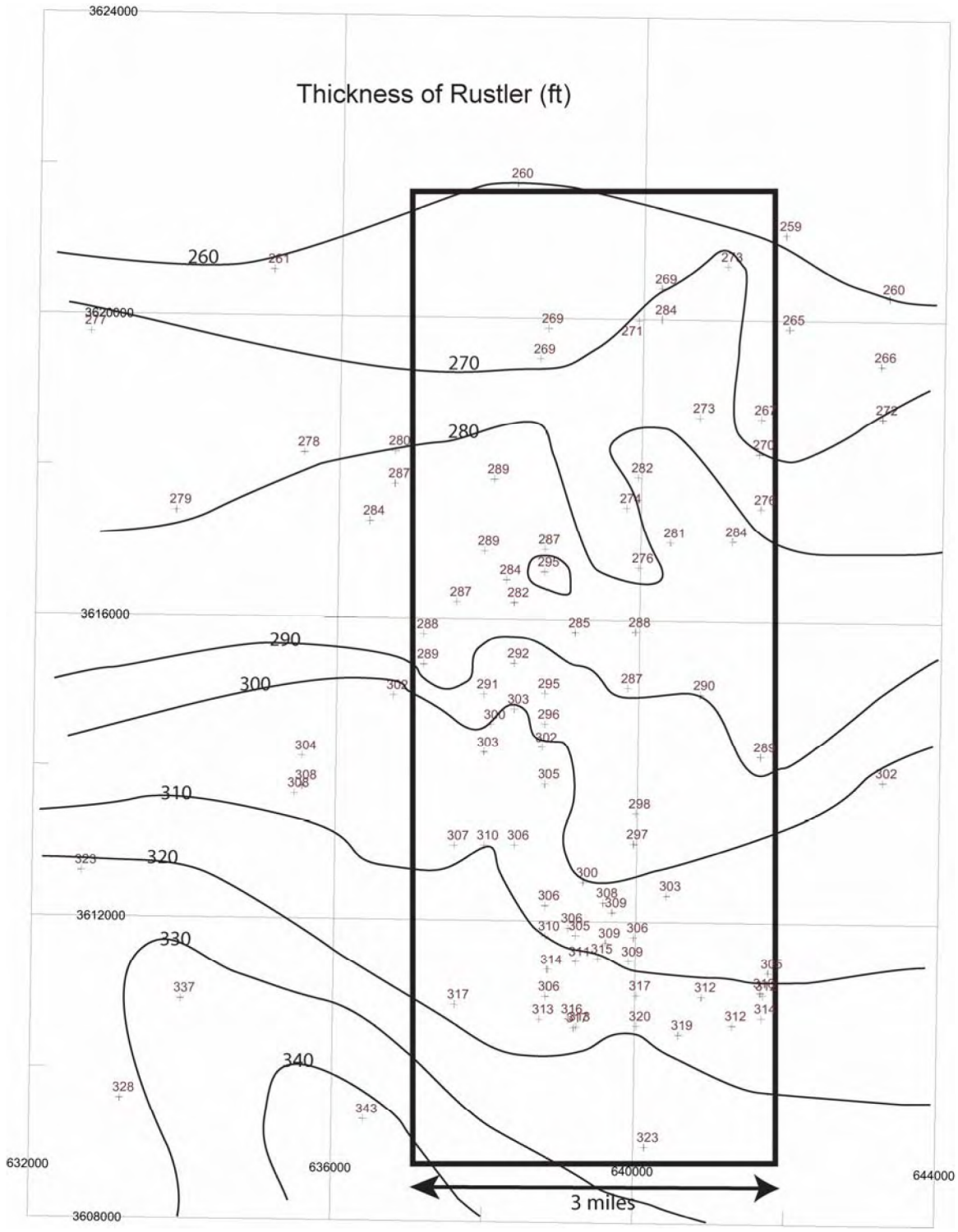

Figure 29 – Thickness (ft) of the Rustler across the trend of the redbed ridge. Gridlines are UTM coordinates (m; Zone 13). Rectangle is shown in Figure 25.

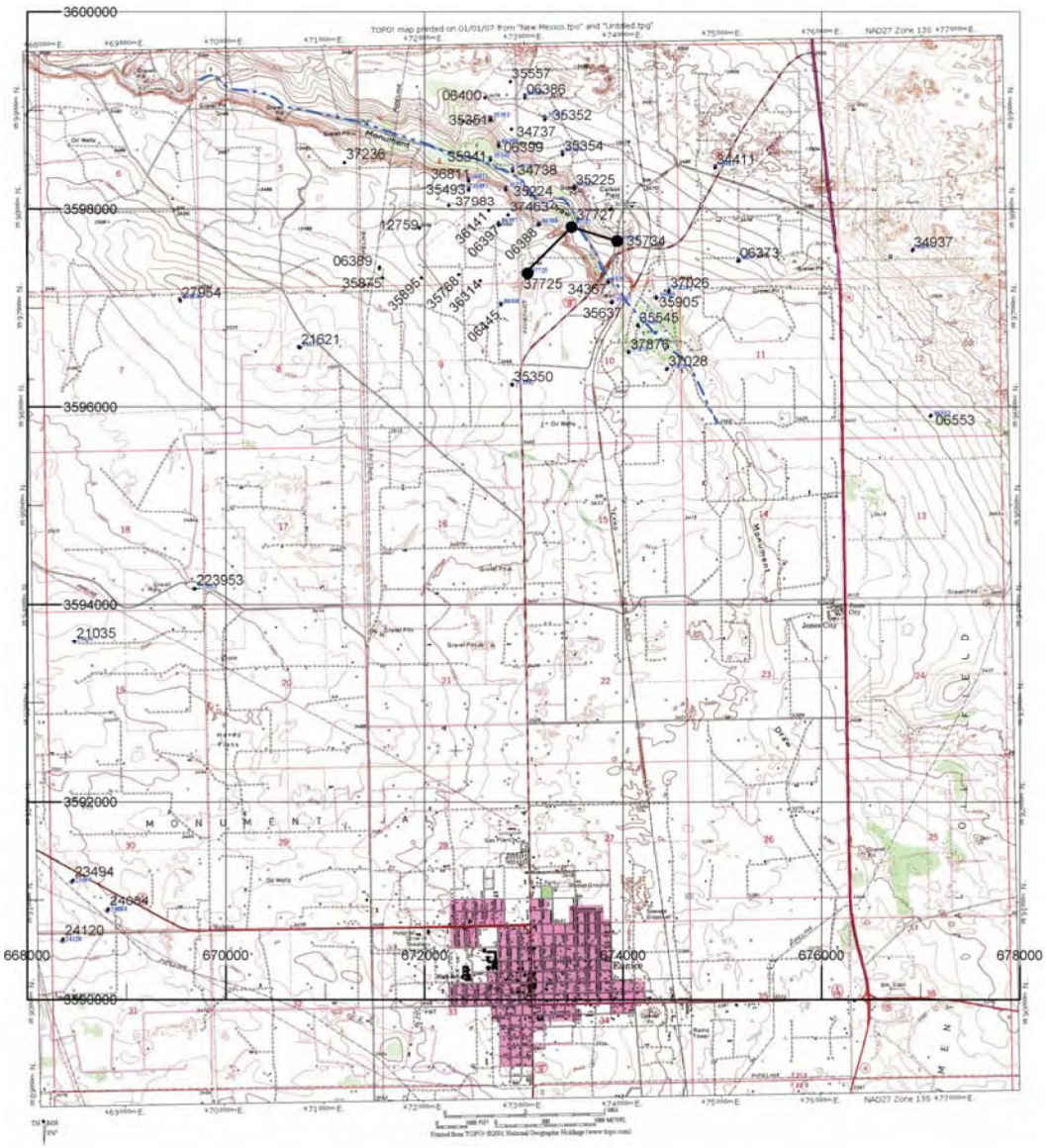

Figure 30 – Topographic base (T21S, R37E) with abbreviated API numbers (add 30-025- to the number) for drillholes for which geophysical logs were interpreted at and around section 3 and the carbon black plant. The dashed blue line indicates the topographic location of the Monument Draw drainage and is repeated in subsequent contour maps. Black overlay lines and values are UTM (NAD27; Zone 13) coordinates in meters with a 2000-m spacing. Three black dots connected by a line is the location of a log section into the draw (Figure 34).

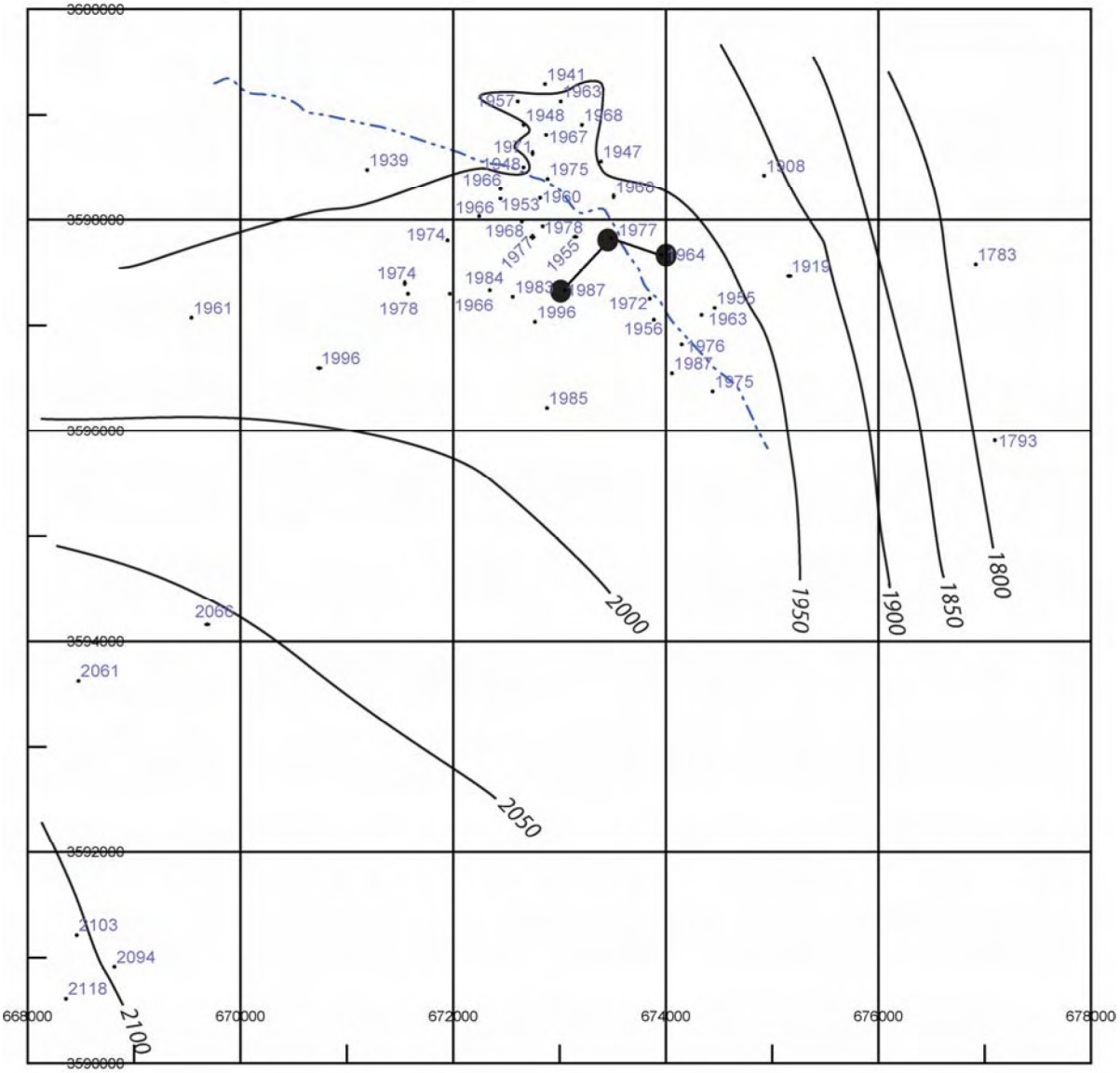

Figure 31 – Elevation (ft amsl) of the top of the Salado Formation in the vicinity of this segment of Monument Draw, NM. Only a few wells were selected at greater distances from section 3 to provide more control on contours. Grid lines show UTM coordinates (m; Zone 13).

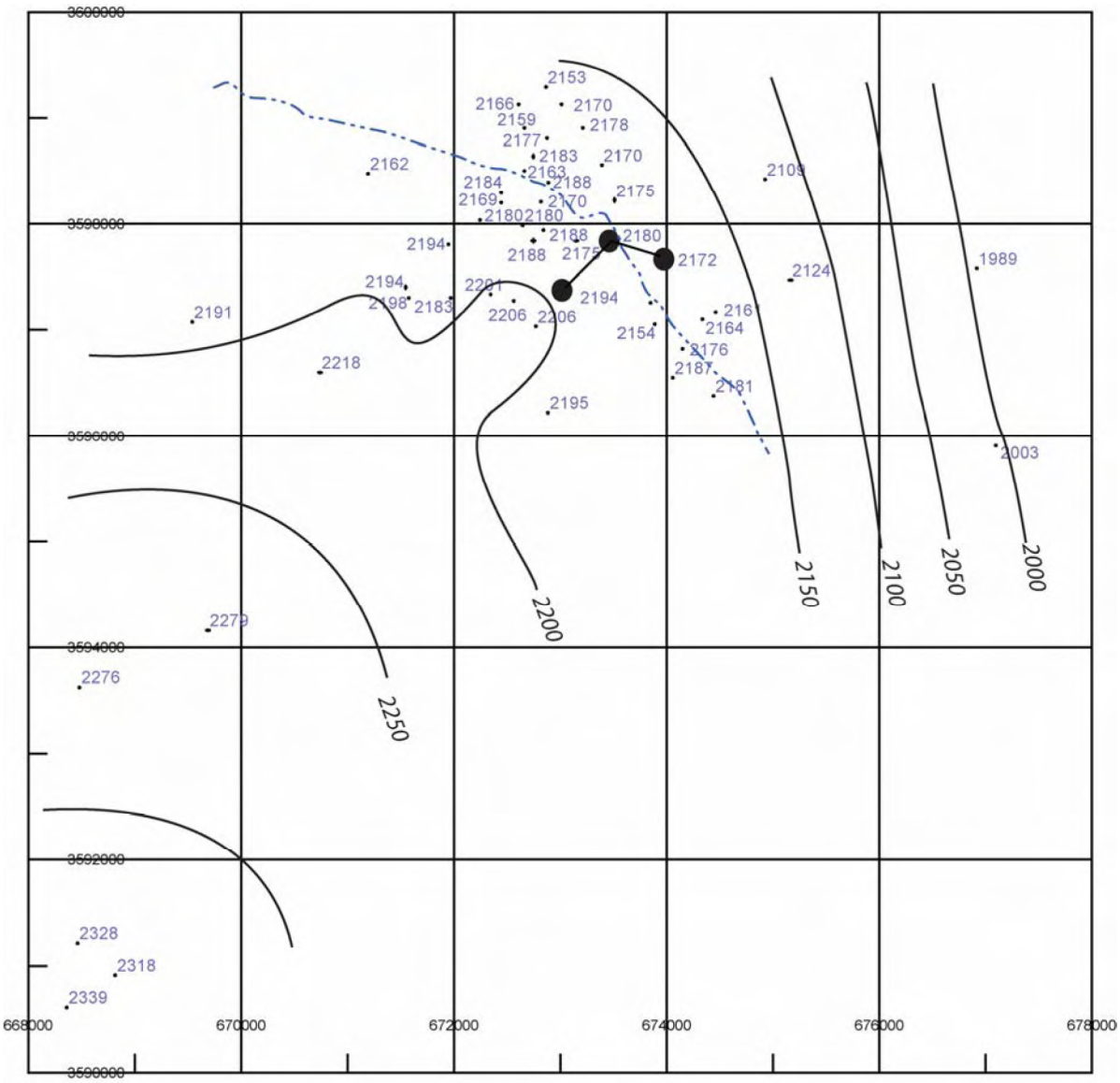

Figure 32 – Elevation (ft amsl) of the top of the Rustler Formation in the vicinity of this segment of Monument Draw, NM. Only a few wells were selected at greater distances from section 3 to provide more control on contours. Grid lines show UTM coordinates (m; Zone 13).

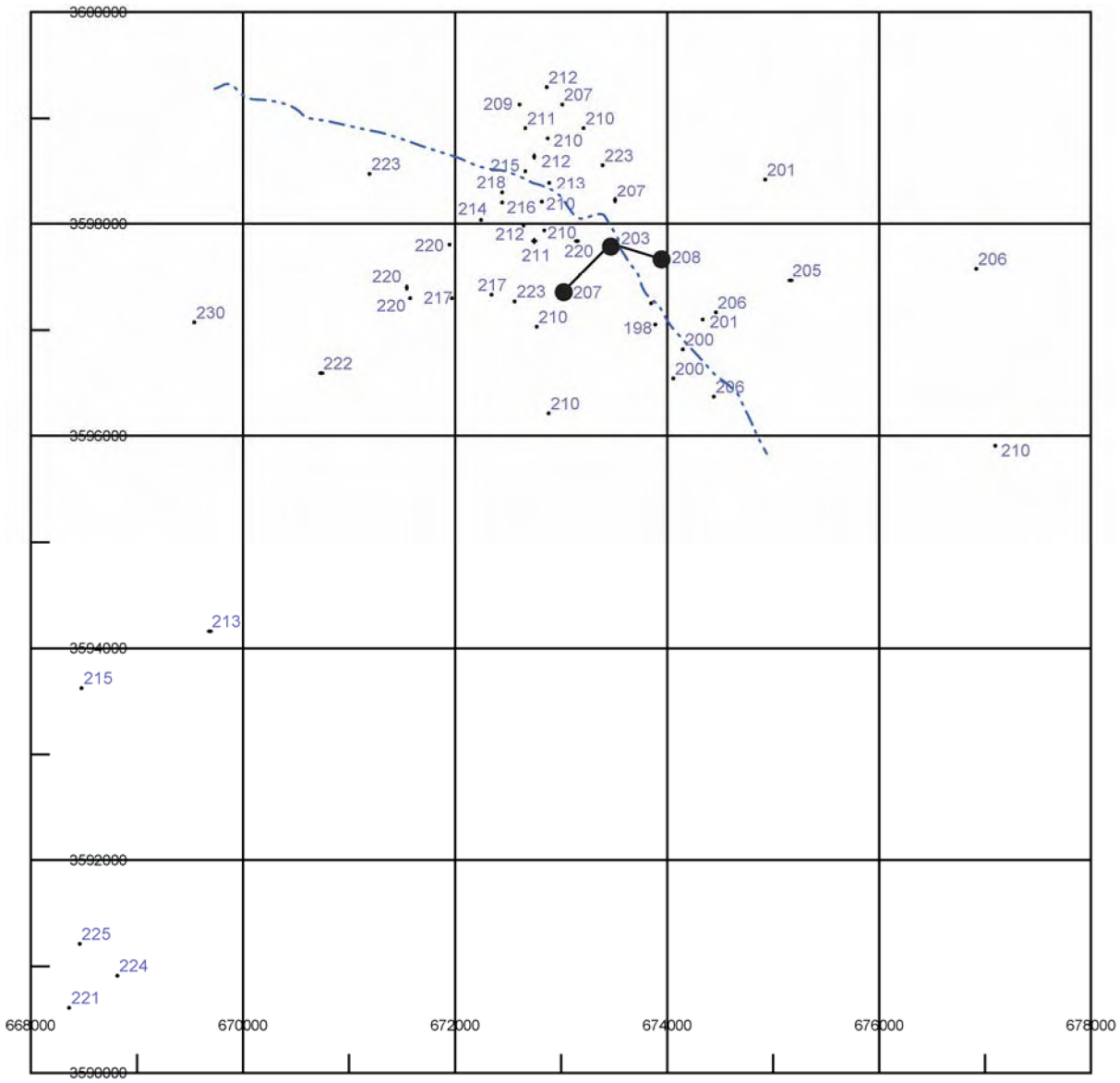

Figure 33 – Thickness (ft) of the Rustler in the vicinity of this segment of Monument Draw, NM. No contours were drawn because of the limited variation. Grid lines show UTM coordinates (m; Zone 13).

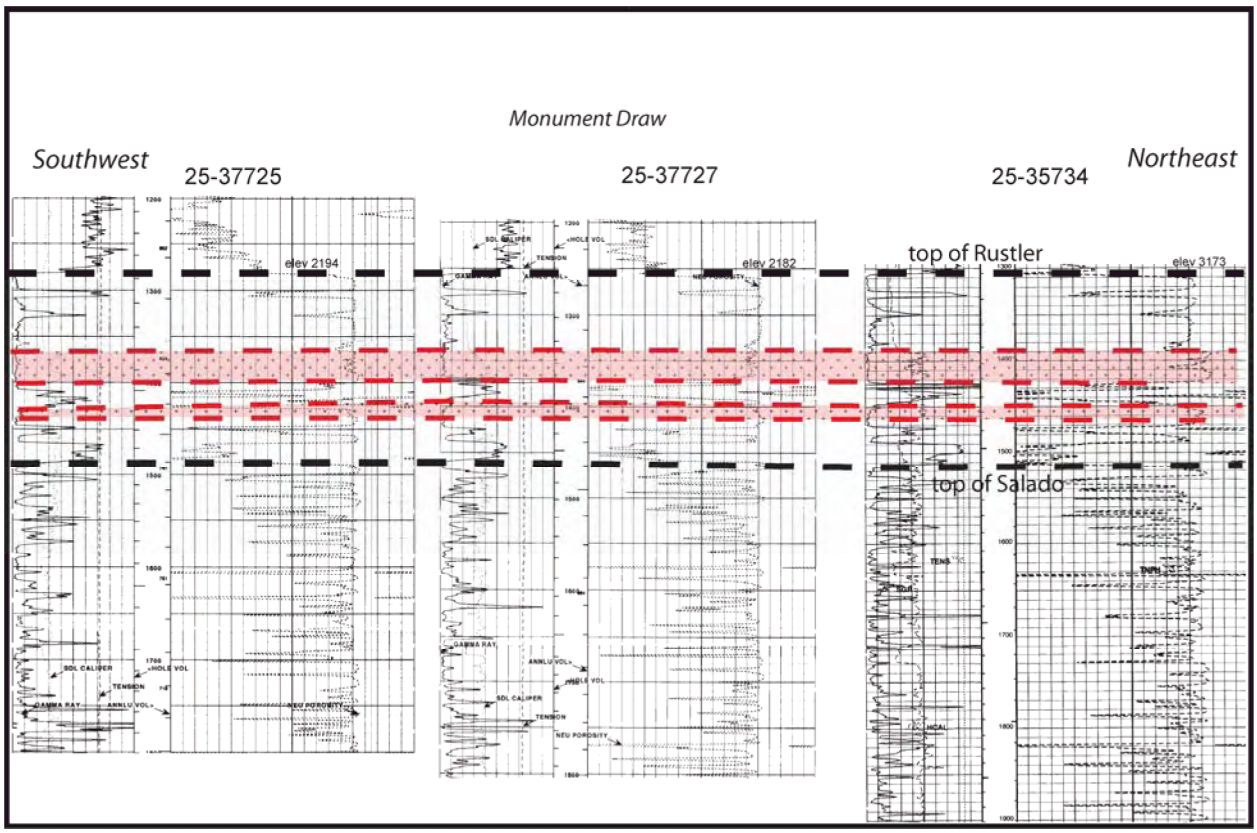

Figure 34 – Geophysical logs (see Figure 30 for location) illustrating little change in thickness for the Rustler and upper Salado from outside Monument Draw to the center and eastern side of the draw. Light red shows halitic zones, the uppermost in this area, are persistent and little changed. The Draw did not develop at its present location in response to solution of this halite and subsequent subsidence.

APPENDIX A

GYPSUM IN REDBEDS AT THE WCS SITE

OCCURRENCE OF GYPSUM AT THE WCS SITE

Outcrops of the Dockum Group in the RCRA landfill at the WCS site contain minor amounts of gypsum. Gypsum appears to be confined to a ~20 ft thick horizon roughly 30 ft below the caliche caprock and is absent from this horizon where calcic alteration has penetrated the upper Dockum surface. The gypsum horizon does not occur throughout the RCRA landfill excavation and is limited to the southern-most outcrops. Gypsum is contained within burrowed, mottled red, silty to sandy mudstone displaying blocky fabrics consistent with paleosol formation and pedogenic movement of clays. Slickensides are also common within the mudstone. Dockum Group cores from the site area show little evidence of gypsum to depths of up to 270 ft, indicating that the gypsum occurs only locally. The gypsum displays a variety of morphologies including fibrous antitaxial veins, lenticular gypsum rosettes, and passive pore-filling cements in fractures. In the following, we discuss describe each of these gypsum morphologies and then comment on its origin.

GYPSUM MORPHOLOGIES

Poorly preserved, discontinuous, arcuate to planar, subvertical to subhorizontal, antitaxial gypsum-filled veins occur within the gypsum-bearing interval at the WCS site (Figure 1). Crystals within the veins are blocky and are primarily oriented perpendicular to the edge of the vein, indicating that minimum principle stresses were oriented subvertically when the veins formed (e.g., Durney and Ramsay, 1973; Ramsay, 1980). Gypsum crystals within the veins appear to be partly corroded or fluted and may show local overgrowths or recrystallization (Figure 2), indicating a complex fluid history since the veins first formed. Medial lines,

commonly associated with antitaxial veins, are poorly preserved due to gypsum dissolution, overgrowth, and possible recrystallization.

At the WCS site, lenticular gypsum rosettes occur in elongated zones along some fractures, in cylindrical zones (possible rizoliths) (Figure 3), and as irregular masses (Figure 4). Gypsum crystals range up to ~1 cm and contain inclusions of the mudstone host rock. The morphology of the gypsum crystals provides some information about their origin. Lenticular gypsum crystals form from alkaline fluids (pH >7.5) in the presence of soluble organic materials at relatively high temperatures (greater than ~ 35° C) (e.g., Cody, 1979; Cody and Cody, 1988). Lenticular penetration twins observed at the WCS site also require the presence of high concentrations of terrestrial humic substances in the pore fluids (Cody and Cody, 1988).

Large (several cm), interlocking gypsum crystals occupy some fractures at the WCS site (Figure 5). Some crystals contain small inclusions of mudstone, while the surfaces of other crystals are lenticular. The large crystal size indicates that most of this gypsum grew passively into and filled existing void space associated with fractures. Limited displacive and incorporative growth may have occurred as the crystals began to encroach on the boundary of previously open fractures.

DISCUSSION

Widespread occurrences of antitaxial gypsum veins have been attributed to stresses induced by large-scale processes such as unloading (Holt and Powers, 1990 a, b; El Tabakh et al, 1998) and collapse due to regional-scale dissolution (Gustavson et al., 1994). The limited vertical and areal extent of gypsum at the WCS site, however, eliminates unloading and dissolution as a potential cause of the gypsum veins found at the site. Because the veins are typically small in

length (< 1 m), discontinuous, subvertical, and often arcuate, they likely developed below the water table in response to localized stress conditions within ductile Dockum mudstones. Under these conditions fracturing is not required to produce antitaxial gypsum veins, as the force of crystallization is sufficient to open the space required by the vein, and the orientation of veins and their fibers reflect local stress conditions (e.g., Means and Li, 2001; Elburg et al., 2002; Hilgers and Urai, 2005). Furthermore, it is difficult to maintain open fractures within a water-saturated mudstone. The original fibrous texture of the veins has been altered by recrystallization and overgrowth, and later gypsum undersaturated fluids dissolved and corroded vein fibers. Because other forms of gypsum are also present within the same limited area, it is likely that these veins developed within the same hydrologic environment as the other forms of gypsum present at the site. This does not represent a new concept as syndepositional gypsum veins have been reported elsewhere (e.g., Holt and Powers, 1990 a,b; Aref and Morsy, 2000).

The forms of gypsum present at the WCS site reveal additional information about the hydrologic system in which they formed. Crystal habits suggest that lenticular gypsum rosettes at the WCS site formed displacively in soft sediments containing warm and alkaline groundwater with high amounts of humic substances (e.g., Cody and Cody, 1988), requiring the decomposition of large amounts of plant matter. The lenticular habit of some of the passive pore-filling crystals suggests that they are coeval with the rosettes and also formed in warm, alkaline, humic-rich groundwater.

The limited extent of gypsum and its proximity to the caliche caprock at the WCS site suggest that hydrologic environments that formed gypsum were also of limited vertical and areal extent. Because abundant humic substances are required to form lenticular gypsum rosettes, the gypsum formed in a shallow, phreatic aquifer in a warm climate with abundant vegetation.

These conditions suggest that the gypsum likely developed beneath or at the margins of a small saline lake or wetland.

The source of dissolved gypsum within the groundwater need not be the deep evaporites that occur over 1,500 ft below the gypsum horizon. Low permeability mudstones separate deeper Dockum aquifers from the gypsum horizon, and current groundwater age dating (Darling, 2006) supports hydrologic separation. During the Triassic and throughout most of the Cenozoic, eastward-draining fluvial systems associated with the Dockum Group and Ogallala Formation crossed evaporite-bearing rocks exposed west and northwest of the WCS site. Groundwaters associated with these fluvial systems were likely to be enriched in dissolved gypsum. Sulfate may also have been derived from sulfide minerals within the Dockum group mudstones (e.g., Joeckel et al., 2005), atmospheric sulfer (e.g., Dultz and Kühn, 2005), Cretaceous seawater, or shallow saline groundwaters associated with saline lakes (e.g., Wood and Jones, 1990).

Gypsum at the WCS site could not have formed in the Holocene. The relationship to pedogenic carbonate indicates gypsum formed earlier than the calcretes. The OAG interval at the WCS RCRA landfill currently contains no groundwater. Nearby, the pH of groundwater in two samples from the OAG aquifer is 7.36 and 7.15 (Darling, 2006), too low to generate lenticular crystals (Cody and Cody, 1988). Furthermore, OAG waters are undersaturated with respect to gypsum, and the vegetative cover cannot provide sufficient humic substances to generate gypsum rosettes.

The gypsum horizon predates the development of the caprock caliche. Gypsum is absent where calcic alteration associated with the caliche caprock has penetrated the upper Dockum surface. The caprock developed on a long stable topography. In the vicinity of topographically low areas, downward percolating fluids dissolved gypsum, reducing the areal extent of the

gypsum horizon. The gypsum horizon was preserved in topographically high areas where gypsum was beyond the depth of high amounts of infiltrating precipitation. Some etching and corrosion of gypsum veins likely occurred during the development of the caprock.

In the vicinity of the WCS site, conditions suitable for the development of warm, alkaline, saline lakes or wetlands bounded by vegetated environments have existed several times prior to the development of the caprock. Dockum mudstone textures observed at the WCS site are consistent with a wetland or a shallow lacustrine environment, and the Dockum environment was sufficiently warm to produce lenticular gypsum. Abundant burrowing attests to significant biological activity, and soil textures suggest subaerial exposure and the presence of plants. During the accumulation of the Dockum, fluvial systems drained evaporite terrains west and northwest of the site (McGowen et al., 1979). Groundwaters associated with these systems were likely sufficiently alkaline and saline to lead to localized gypsum accumulation in the vicinity of wetlands and lakes. These conditions persisted after Dockum deposition. Eastward drainage of evaporite terrains likely continued after Dockum deposition until the accumulation of the Antlers Formation during the Cretaceous. While this period of time is dominated by net erosion, localized wetlands or saline lakes capable of accumulating the WCS gypsum may have developed. During the Cenozoic, eastward drainage over evaporite terrains again resumed, and localized wetlands or saline lakes could have formed.

SUMMARY

There are three major summary points from this examination of gypsum occurrences at the WCS site and a review of literature:

- Because the gypsum is limited in areal extent and occurs within a limited horizon near the upper surface of the Dockum redbeds, the occurrence of gypsum cannot be related to large-scale processes such as unloading or dissolution of underlying evaporites.
- Antitaxial gypsum vein morphologies suggest that the veins developed in response to localized stress conditions.
- Gypsum morphologies indicate formation in shallow, warm, alkaline groundwaters. The most likely setting and time of formation is syndepositional, as sulfate, organic activity, and warm temperatures should have been present at and near the surface; other possible periods of exposure or near-exposure occurred between Dockum deposition and the deposition of the Cretaceous Antlers Formation and in the Cenozoic prior to the accumulation of the caprock.

REFERENCES

Aref, M. A., and M. A. Morsy, 2000, Polygonal shrinkage cracks filled with gypsum in the Upper Eocene, Fayum, Egypt, *Sedimentology of Egypt*, vol. 8, p. 89-103.

Cody, R. D., 1979, Lenticular gypsum: Occurrences in nature, and experimental determinations of effects of soluble green plant material on its formation, *Journal of Sedimentary Petrology*, vol. 49, no. 3, p. 1015-1028.

Cody, R. D., and A. M. Cody, 1988, Gypsum nucleation and crystal morphology in analog saline terrestrial environments, *Journal of Sedimentary Petrology*, vol. 58, no. 2, p. 247-255.

Darling, B. K., 2006, Letter report on findings related to the age-dating of groundwater at a proposed treatment and disposal facility for low-level radioactive waste, Andrews County, Texas, *unpublished report*, LBG-Guyton Associates, Lafayette, LA.

Durney, D. W. and Ramsay, J. G., 1973, Incremental strains measured by sysntectonic crystal growths, in *Gravity and Tectonics*, K.A. de Jong and R. Scholten (eds), John Wiley and Sons, New York, p. 67-96.

Dultz, S. and P. Kühn, 2005, Occurrence, formation, and micromorphology of gypsum in soils from the Central-German Chernozem region, *Geoderma*, vol. 129, p. 230-250.

El Tabakh, M., B. C. Schreiber, and J. K. Warren, Origin of fibrous gypsum in the Newark Rift Basin, Eastern North America, *Journal of Sedimentary Research*, vol. 68, no. 1, p. 88-99.

Elburg, M. A., P. D. Bons, J. Foden, and C. W. Passchier, 2002, in *Deformation mechanisms, rheology and tectionics: Current status and future perspectives*, S. de Meer, M. R. Drury, J. H. P. de Bresser, and G. M. Pennock (eds), Geological Society, London, Special Publications, vol. 2000, p. 103-118.

Gustavson, T. C., S. D. Hovorka, and A. R. Dutton, 1994, Origin of satin spar veins in evaporite basins, *Journal of Sedimentary Research*, vol. 64, no. 1, p. 88-94.

Hilgers, C., and J. L. Urai, 2005, On the arrangement of solid inclusions in fibrous veins and the role of the crack-seal mechanism, *Journal of Structural Geology*, vol. 27, p. 481-494.

Holt, R.M., and D. W. Powers, 1990a, Geotechnical activities in the air intake shaft (AIS): *DOE/WIPP 90 051*, US Department of Energy, Carlsbad, NM.

Holt, R.M., and D. W. Powers, 1990b, The Late Permian Dewey Lake Formation at the Waste Isolation Pilot Plant, in Geological and Hydrological Studies of Evaporites in the Northern Delaware Basin for the Waste Isolation Pilot Plant (WIPP), D.W. Powers, R. M. Holt, R. L. Beauheim, and N. Rempe, (eds) Guidebook 14, Geological Society of America (Dallas Geological Society), p. 45-78.

Joeckel, R. M., B. J. Ang Clement, L. R. VanFleet Bates, 2005, Sulfate-mineral crusts from pyrite weathering and acid rock drainage in the Dakota Formation and Graneros Shale, Jefferson County, Nebraska, *Chemical Geology*, 2005, vol. 215, p. 433-452.

McGowen, J. H., G. E. Granata, and S. J. Seni, 1979, Depositional framework of the lower Dockum Group (Triassic) Texas Panhandle, *Report of Technical Investigations No. 97*, Bureau of Economic Geology, The University of Texas at Austin, 60 p.

Means, W. D., and T. Li, 2001, A laboratory simulation of fibrous veins: Some first observations, *Journal of Structural Geology*, vol. 23, p. 857-863.

Ramsay, J. G., 1980, The crack-seal mechanism of rock deformation, Nature, vol. 284, p. 135-139.

Wood, W. W. and B. F. Jones, 1990, Origin of solutes in saline lakes and springs on the southern High Plains of Texas and New Mexico, in *Geologic framework and regional hydrology; upper Cenozoic Blackwater Draw and Ogallala Formations, Great Plains*, T. C. Gustavson (ed), proceedings of the Symposium on geology and geohydrology of the Tertiary Ogallala Formation (Group) and Quaternary Blackwater Draw Formation, Lubbock, TX, p. 193 – 208.

APPENDIX A FIGURES